DESIGN AND PERFORMANCE OF THE NLCTA-ECHO 7 UNDULATORS

Stephen Gottschalk, Robert Kelly, Michael Offenbacker, John Zumdieck STI Optronics, Bellevue, WA 98004, USA

Abstract

The Echo-enabled harmonic generation (EEHG) FEL at SLAC NLCTA has shown coherent radiation in the seventh harmonic (227 nm) of the second seed laser [2]. Earlier experiments demonstrated 3rd and 4th EEHG [1]. We describe design and performance of the 33-mm and 55-mm period undulators built by STI Optronics and used for these experiments. Magnetic design of the 33-mm period undulator was based on an earlier curved-pole, two-plane focusing undulator for the UCLA seeded THz FEL [3]. The 55-mm undulator was identical to the JLAB IR FEL and APS UA U55 designs. A challenge for both these devices was achieving tight normal and skew trajectory excursions (<500 G-cm^2), zero trajectory offset and <10 G-cm steering without end correctors over a 5-mm diameter horizontal and vertical region with a 4-month delivery requirement. We will also describe a new tuning method based on operations research linear programming that was used to help meet these goals over a 2X larger region while maintaining 1° phase errors.

INTRODUCTION

EEG enables seeded X-ray FELs without the shot noise limitation of SASE mode. The theory of EEG is summarized in [1] and advantages of EEG for achieving temporally coherent X-ray operation are described in [2]. The EEG FEL at the NLCTA at SLAC has demonstrated 7th harmonic operation at 227 nm with a 120-MeV electron beam using 795-nm and 1590-nm seed lasers [2]. The experiments utilize multiple chicanes, undulators, and transverse rf cavities. For this project we made undulators U1 (10 periods, 3.3-cm period) and U2 (10 periods, 5.5-cm period) to the specifications shown in Table 1. One device was a modified 33-mm period undulator [3] in which the two-plane sextupolar focusing was replaced by flat pole, one-plane focusing while the 55-mm period device was the same as APS Undulator A, 55 mm and JLAB IR 55 mm. Fig. 1 shows the 55-mm period undulator at NLCTA and the 33-mm period device during scanning at STI.

Table 1: EEHG Undulator Performance

Item	U1 Specification	U1 Actual	U2 Specification	U2 Actual
Type	Hybrid	Hybrid	Hybrid	Hybrid
Magnetic Material	Not specified	Vacodym 890TP Br = 1.164T	Not specified	Shin-etsu N32Z BR = 1.11T
Gap	>10 mm	10.653 mm	>10 mm	25.47 mm
Wiggle Plane	Horizontal	Horizontal	Horizontal	Horizontal
Good Field Region	2.5-mm radius	-3 mm to >5 mm	2.5-mm radius	-4.5 mm to >5 mm
Number of Full Strength Periods	9.5	10.5	9.5	10.5
Period Length	33mm	33.013 mm	55 mm	55.035 mm
K	1.8016	1.8018	2.0724	2.0722
Peak Field	0.5845T	0.5846T	0.4034%	0.40336
First Integrals in Good Field Region	<10 G-cm (x,y)	-5.9 to -6.0 skews +5 to -10 normals	<10 G-cm	-3.0 to -8.0 skews 0 to -6.0 normals
Second Integrals in Good Field Region	<1000 G-cm^2	80 to -50 skews 400 to 0 normals	<1000 G-cm^2	560 to 300 skews 300 to 550 normals
Transverse Rolloff	<1% at 5 mm	0.7%	<1% at 5 mm	0.3%
Pole Width	Not Specified	25.58 MM	Not Specified	55 mm
Phase Error	<20°	0.8°	<20°	1.1°

Figure 1: 55 mm (left, on NLCTA) and 33 mm (right, being scanned) period undulators.

MAGNETIC DESIGN

Central and End Fields

Both undulators used ultra-high coercivity magnets to maximize radiation resistance. The 33-mm period magnets were Vacuumschmelze Vacodym 890TP with Br = 1.164T, Hc,J > 1598 kA/m at 20 °C, Br = 1.11T, Hc,J = 1097 kA/m at 150 °C, based on hysteresigraph data. For the 55-mm period undulator the magnets were Shin-Etsu N32EZ with Br = 1.12T at 20 °C (based on Helmholtz coil data). Straight poles provided sufficient field strength and allowed re-use of earlier designs.

End fields were standard reduced magnet height, reduced pole height designs [4]. Since the trajectory offset requirement was 100X smaller than APS UA, extra care was needed when setting the end pole and magnet sizes. Parametric mesh settings, polynomial order values and sensitivity analyses were used. For the 33-mm period end fields we used the OptiNet evolutionary optimizer from Infolytica Corp to run the parametric end field FEA analyses. Our scripts calculate wiggle averaged 1st and 2nd integrals and OptiNet parametrically changed magnet and pole sizes to achieve zero steering, zero offset, maximum number of full strength poles without overshoot at the 4th pole in an automatic manner. Typical optimizations require 100-300 3D FEA runs. The 33-mm period end field is shown in Fig. 2.
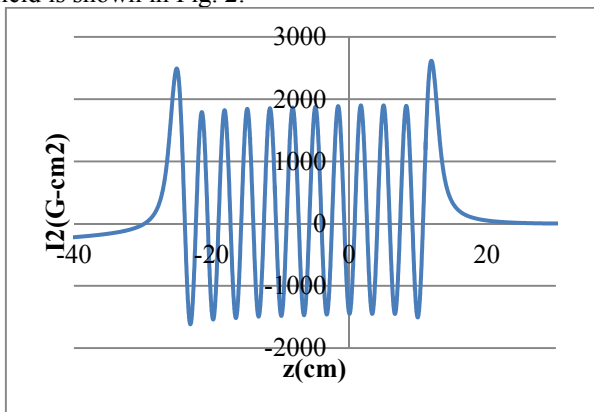
Figure 2: Calculated 33-mm period end field.

However, we encountered difficulty with the 55-mm end optimization. It would have required much smaller nonlinear solver tolerances leading to significantly longer optimization times than allowed in the schedule. Therefore, we used a variation of Richardson's extrapolation [5] for signature functions. In this approach, the changes in B-field caused by adjustments of pole or magnet heights are found for two different finite nonlinear solver tolerance settings. Then the B-field change vs. z is extrapolated to zero tolerance. A fast optimizer (we used the SOLVER add-in for Excel) quickly calculated quantities of interest and optimized the design. The signature functions from this extrapolation approach are shown in Fig. 3 along with a scaled B-field for reference. These signature functions also permit determination of sensitivity matrices.
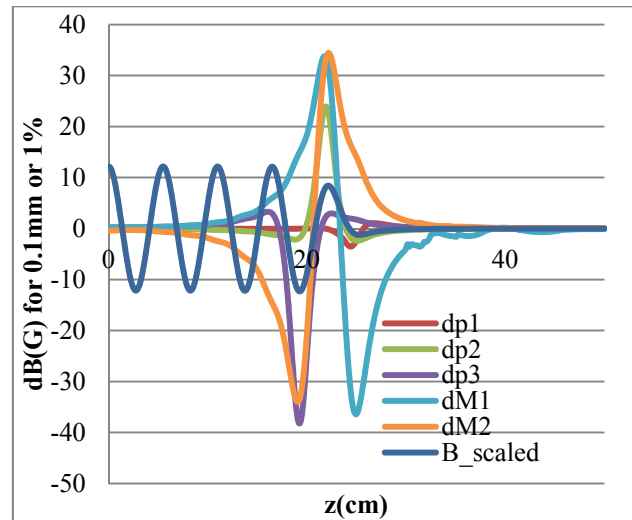
Figure 3: 55-mm period undulator end field signature functions.

We found that 0.1 mm or 1% strength changes easily cause 1% peak field changes for the 3rd pole, 50 G-cm changes in the 1st integrals and 800 G-cm^2 changes to the 2nd integrals. Finally, the FEA parameters are adjusted to match the SOLVER estimates and the FEA model is solved with MagNet to confirm the results.

Ambient Fields

Environmental magnetic fields are modified by ferromagnetic material such as steel in linear guides and

rails, strongbacks and (for hybrid undulators) the poles. We have found that every undulator has a unique ambient field signature and per requirements, we removed our ambient field from the scans prior to tuning. The approach is to import a 3D CAD file of a half wiggler into Magnet, apply the appropriate boundary conditions and material properties and then add a uniform 1-G external B-field. The resulting gap dependent skew and normal ambient fields are then used to subtract the STI ambient fields. Multipoles were analysed and found to be small. About 15% of the skew remains (Fig. 4). The normal ambient signatures are more complex and show evidence of the linear guides.
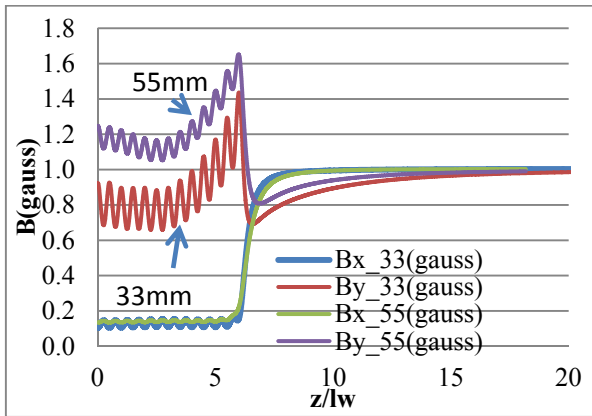
Figure 4: Ambient field signatures.

MECHANICAL DESIGN

While the requirements in Table 1 are at one gap, the magnetic field strength was specified to within 1 G, which implies 1.8 μ (33 mm) to 4.3 μ (55 mm) accuracy in the gap. We used a non-backdriving Acme screw jack shown in Fig. 1 and a 1-μ resolution digital micrometer to adjust the upper beam while the lower beam used a linear guide mounted stop and a spring preload. Crossed roller guides were used to hold each magnetic assembly. A safety hard stop (not visible in Fig. 1) was also included. The vertical and horizontal mounting plates were MIC-6 ground aluminum with an aluminum angle bracket to achieve perpendicularity. Beams were aligned axially and transversely during assembly to minimize cant and pole axial and transverse skew. The horizontal plates used adjustable kinematic mounts (cone, V, flat). Beams used 8 tooling balls at fiducialized locations plus redundant gage pad readings at 8 locations, pole scribe lines and ceramic gage block values for end poles. Rough alignment used bubble levels at reference locations plus a jig transit while fine alignment (few microns) used magnetic scan analyses.

OPERATIONS RESEARCH TUNING APPROACH AND MEASURED PERFORMANCE

Trajectory and phase tuning of the 33-mm period undulator used spreadsheets developed for APS Undulator A. Multipole shims were located so that the trajectory multipoles were tuned at the same time as the integrated multipoles. This requirement is becoming more typical for FEL's which need to maintain optical beam overlap. Performance is shown in the upper part of Fig. 5. The sextupole for the undulators was the result of the symmetric B-field specification coupled with the natural sextupole of the finite width poles. This was larger on the 33mm period device because it had smaller poles.

For the 55-mm period undulator we developed a tuning algorithm based on operations research integer programming. Global optimization falls into two broad categories: exact methods for small problems and "good enough" heuristic methods (simulated annealing, evolutionary, genetic, ANT) for large problems. Short undulators like these fall into the small problem category. For optimization with linear objectives but continuous variables the Simplex algorithm [5] is a good choice for small problems while integer programming using branch and bound [6] is the preferred method with discrete variables. As noted in [6] for some integer programming problems, a rounding of continuous variable approach generates poor or even infeasible optimization results. Shim thicknesses are discrete and we found on NISUS [7] that rounding continuous shim thicknesses introduced errors that required further iteration.

An additional subtlety for short undulators is that because of end effects, shim signature functions are not shift-invariant. They are different for each shim. Field changes were a convolution of individual shim signatures functions for every location in the undulator.

Finally, the symmetric design did not cancel quadrupoles caused by small cant angles, so normal quadrupole shimming was needed.

We used the commercial integer programming package What's Best (www.lindo.com). An Excel spreadsheet was used to predict performance when arbitrary shim thicknesses are used. The optimizer adjusted thicknesses subject to positive total shim thickness, I1 and I2 constraints while minimizing trajectory fluctuations. Trajectory shimming was interleaved with normal and skew multipole shimming to meet the requirements in Table 1. Results are shown in the lower plots of Fig. 5.
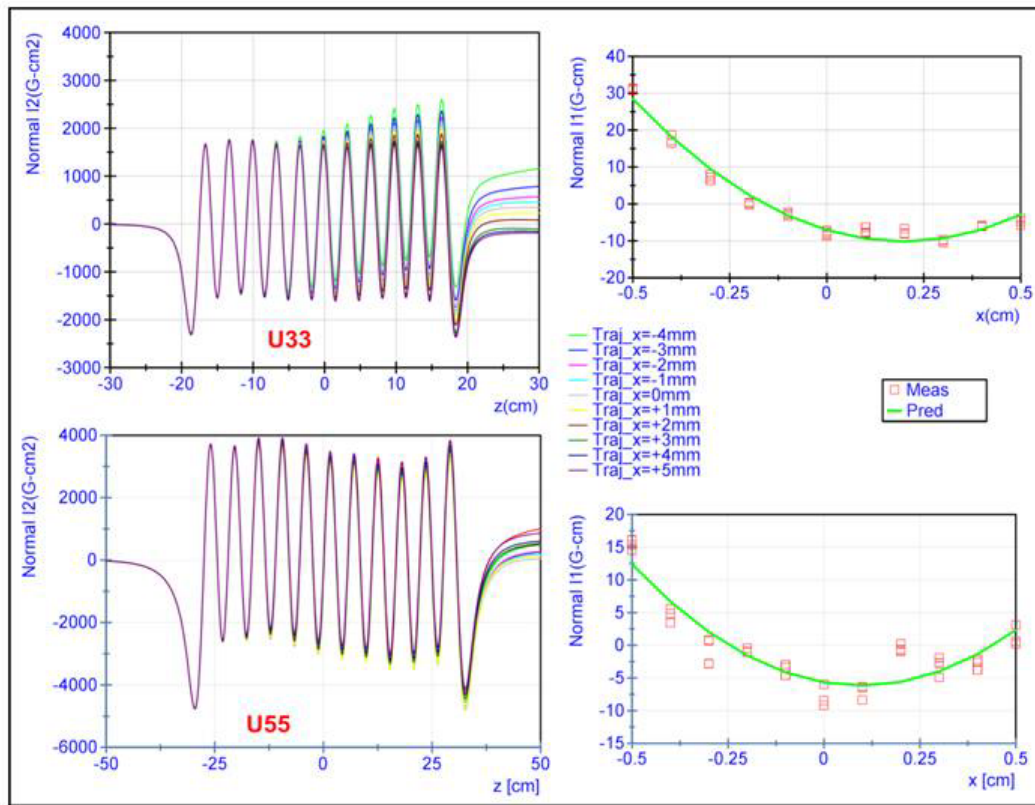
Figure 5: 33 and 55mm period performance.

CONCLUSION

We have described approaches used to achieve the requirements of the Echo-7 undulators. End field and tuning algorithms have been discussed which are generally applicable to FEL undulators.

ACKNOWLEDGEMENTS

REFERENCES

[1] D. Xiang et al, Phys. Rev. Letters 105 114801 (2010)

[2] D. Xiang et al, Phys. Rev. Letters 108 024802 (2012)

[3] S. Gottschalk et al, "UCLA Seeded THz FEL Undulator-Buncher Design", WEPD68 these proceedings.

[4] S. Gottschalk, et al, "Zero Displacement End Termination of Undulators and Wigglers", PAC99, p. 2674-2676.

[5] Press W, Flannery B, Teukolsky S, Vetterling, "Numerical Recipes-The Art of Scientific Programming (Fortran version)", Cambridge University Press NY (1989).

[6] M. Trick, "A Tutorial on Integer Programming" (1997). http://mat.gsia.cmu.edu/orclass/integer/integer .html

[7] Quimby, et al, "Development of a 10-meter Wedge-Pole Undulator", NIM in Phys. Res. A285 (1989) 281-289.